J. Phys.: Condens. Matter **21** (2009) 335802 (12pp) doi:10.1088/0953-8984/21/33/335802

Interface gap states and Schottky barrier inhomogeneity at metal/n-type GaN Schottky contacts

M Mamor

Physics Department, College of Science, Sultan Qaboos University, PO Box 36 Muscat 123, Sultanate of Oman

E-mail: mamor@squ.edu.om

Received 22 June 2009, in final form 6 July 2009
Published 24 July 2009
Online at stacks.iop.org/JPhysCM/21/335802

Abstract

The barrier heights (BH) of various metals including Pd, Pt and Ni on n-type GaN (M/n-GaN) have been measured in the temperature range 80–400 K with using a current–voltage (I–V) technique. The temperature dependence of the I–V characteristics of M/n-GaN have shown non-ideal behaviors and indicate the presence of a non-uniform distribution of surface gap states, resulting from the residual defects in the as grown GaN. The surface gap states density N_{ss}, as well as its temperature dependence were obtained from the bias and temperature dependence of the ideality factor $n(V, T)$ and the barrier height $\Phi_{Bn}(V, T)$. Further, a dependence of zero-bias BH Φ_{0Bn} on the metal work function (Φ_m) with an interface parameter coefficient of proportionality of 0.47 is found. This result indicates that the Fermi level at the M/n-GaN interface is unpinned. Additionally, the presence of lateral inhomogeneities of the BH, with two Gaussian distributions of the BH values is seen. However, the non-homogeneous SBH is found to be correlated to the surface gap states density, in that Φ_{0Bn} becomes smaller with increasing N_{ss}. These findings suggest that the lateral inhomogeneity of the SBH is connected to the non-uniform distribution of the density of surface gap states at metal/GaN which is attributed to the presence of native defects in the as grown GaN. Deep level transient spectroscopy confirms the presence of native defects with discrete energy levels at GaN and provides support to this interpretation.

(Some figures in this article are in colour only in the electronic version)

1. Introduction

Group III-nitride are attractive compound semiconductors for a wide variety of optoelectronic and microelectronic device applications, such as GaN-based light-emitting diodes (LEDs) and laser diodes (LDs), ultraviolet (UV) detectors and high temperature, high power and high frequency electronic devices. For more detailed information, the reader is referred to the reviews that have already appeared on this subject [1–4]. Such applications often require metallization, thus making the study of the metal/GaN interface extremely important. Indeed, high quality ohmic and rectifying contacts are directly connected to the enhanced performance of GaN-based optoelectronic and electronic devices.

A good metal (M)/n-type GaN Schottky barrier formation requires a metal with a high work function (Φ_M), that is larger than the work function (Φ_s) of the GaN semiconductor, while a metal with low Φ_m is required for the ohmic contacts. Besides satisfying the above requirements for ohmic and Schottky contacts, some problems related to the contacts M/GaN reside principally in defects located near the semiconductor surface with energy levels in the semiconductor band gap [5, 6]. These can be native defects due to deviations from stoichiometry, such as vacancies and antisites. In fact, one can essentially distinguish between two types of defects: (i) defects related to the as grown semiconductor, such as residual structural defects and dislocations, and (ii) those related to the contact between metal and semiconductor. It should be noted that these two types of defects are interdependent. On the one hand, reaction can take place at the metal/semiconductor interface formed during the metal deposition, resulting in the formation of interfacial layer. This results in a configuration like a

metal-interfacial layer-semiconductor with the formation of interface states at the M/n-GaN contact and hence deviating from the expected metal–semiconductor (M/Sc) counterpart. On the other hand structural defects at and below the surface of the Sc, as well as metal-induced gap states (MIGS) [6, 7], result in the formation of surface states in the band gap of Sc. In such a case, the interfacial layer separating the metal from the region of the bulk defects is the semiconductor itself. Such surface states might result in the pinning of the Fermi level at the energetic position of the defects [8] and reduce the performance of GaN-based electronic and optical devices. Since the electrical characteristics of the Schottky contact are controlled mainly by its interface properties, the study of interface states is essential for the understanding of the electrical properties of Schottky diodes (SD). Gaining an understanding of the behavior of such surface states at the GaN and close to the metal/GaN interface, as well as their effect on the respective electrical characteristics of the M/GaN diode, is of fundamental and technological importance for developing GaN-based devices.

Most studies of Schottky diodes formed on n-GaN were limited to the determination of the Schottky barrier height (SBH) at room temperature (RT) by measuring either the capacitance–voltage (C–V) characteristics or the forward current–voltage (I–V) characteristics of the diodes [9–12]. Important additional information can be gained from the temperature dependence of the forward I–V characteristics. It allows the identification of the different conduction mechanism modes across the M/GaN interface and the study of different effects, such as barrier inhomogeneities and surface states density, on carrier transport at M/GaN Schottky barrier diodes (SBDs). In previous works [13, 14], analysis of temperature-dependent I–V characteristics of Schottky diodes formed on n-GaN was used to elucidate a possible conduction mechanism at the metal/GaN interface. However, some authors [15–17] have recently reported the variation of the Schottky diodes parameters of Pt/n-GaN SD with temperature and found a decrease of the SBH and an increase of the ideality factor with decreasing temperature. These results have been explained on the basis of a thermionic emission (TE) mechanism with lateral inhomogeneities at the M/n-GaN interface. However, their analysis of temperature-dependent I–V characteristics was limited only to a certain high temperature range (300–448 K).

In this paper, the temperature-dependent I–V measurements have been extended to the low temperature range (80–400 K) in order to elucidate a possible mechanism of carrier transport at the M/n-GaN SD at lower temperature. On the other hand, the temperature dependence of the electrical characteristics of Schottky contacts fabricated on n-GaN was investigated to extract the density of interface states (N_{ss}) and their features versus temperature. Two different approaches to determine N_{ss} have been considered. The first one is based on the variation of ideality factor (n) with forward applied voltage (V) and temperature. The second approach is based on the variation of the SBH at a given bias as a function of the metal work function. For such a purpose, three different metals (Pd, Ni and Pt) with different Φ_m have been studied. The SBH versus Φ_m only gives information about the density of interface states, while, the variation of n versus V gives information about both N_{ss} and its energy distribution in the band gap. In this paper the temperature-dependent Schottky barrier characteristic is also discussed in terms of the model of inhomogeneities of Schottky contact with a Gaussian distribution of the barrier height (BH). Furthermore, the residual defects in as grown GaN as determined from deep level transient spectroscopy (DLTS) were indicated as one of the possible physical causes of the experimentally observed electrical behavior of the M/n-GaN SD. The associations of various defects contribute to the introduction of surface states in the band gap and SBH inhomogeneities. An attempt has been made to find out any correlation between residual defects, formation of interface states and SBH inhomogeneities at M/n-GaN contacts.

2. Experimental details

GaN epitaxial layers with a free carrier density of (2–3) $\times$ 10^{17} cm^3 and a 1200 nm thickness, grown on a (0001) Al_2O_3 c-plane substrate by metalorganic chemical vapor deposition (MOCVD), were used for this study. Before ohmic contact fabrication, the samples were cleaned [18] by first boiling them in aqua regia and rinsing in deionized water, then a degreasing process followed by boiling in trichloroethylene, then rinsing in boiled isopropanol and thereafter in deionized water. Finally, the samples were dipped in HCl:H_2O (1:1) for 10 s. After this cleaning, Ti/Al/Ni/Au (150 Å/2200 Å/400 Å/500 Å) ohmic contacts [19] were fabricated on the GaN and annealed at 500 °C for 5 min in Ar. Prior to Schottky barrier diode fabrication, the samples were again degreased and dipped in an HCl:H_2O (1:1) solution. Following this, circular metal Schottky contacts 0.66 mm in diameter and 120 nm in thickness were successfully fabricated. Various metals Pd, Ni and Pt with different work functions (5.12, 5.15 and 5.65 eV, respectively) were deposited on n-type GaN through a metal contact mask to serve as Schottky contacts. Temperature-dependent I–V measurements on M/n-GaN SBDs were carried out in the range 80–400 K. Deep level transient spectroscopy (DLTS) measurements were finally carried out in the temperature range 60–400 K. The sample structure and diode configuration are shown in figures 1(a) and (b), respectively.

The Ti/Al/Ni/Au contacts show good ohmic behavior. From the I–V characteristic of the ohmic contacts the resistance is determined to be on the order of 12 Ω. The measured resistance is consistent with the calculated sheet resistance using the equation $R = \rho L/S = L/(\mu_o N_D q S)$, where L is the thickness of the sample, S is the Schottky contact cross-sectional area, μ_o is the electron mobility, and q is the electron charge.

3. Results and discussion

3.1. Extraction of Schottky diode parameters

The forward I–V characteristics, plotted in figure 2 as function of temperature, show an example of the results obtained for

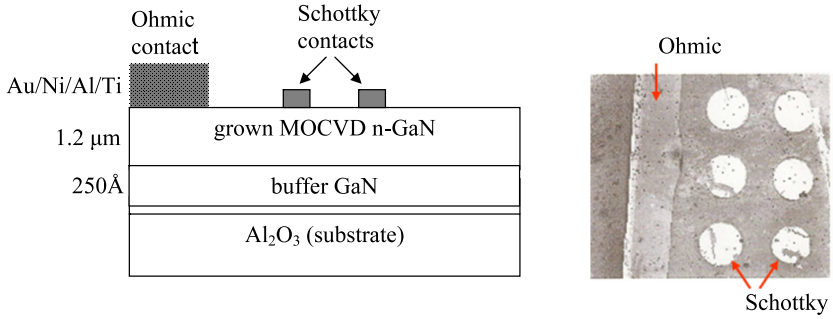

Figure 1. A schematic of the diode structure. (a) Cross-sectional view, (b) top view.

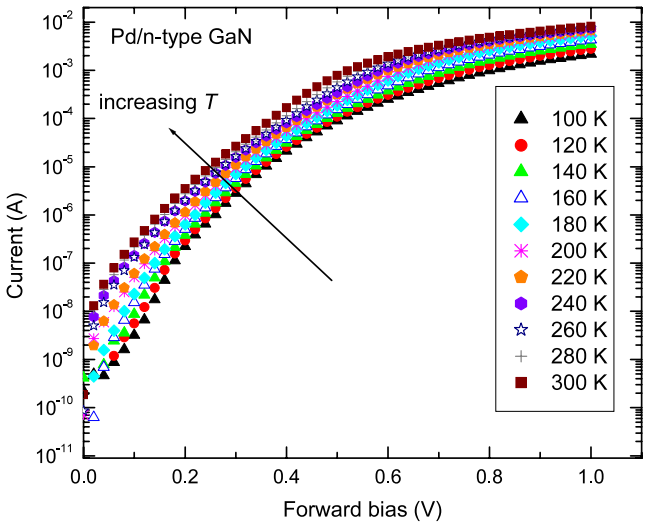

Figure 2. Semi-logarithmic plot of forward I–V characteristics for Pd/n-GaN Schottky diodes as function of the measurement temperature.

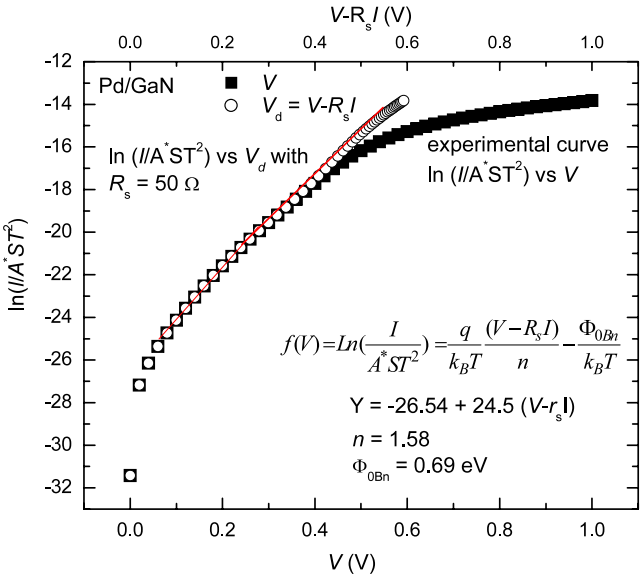

Figure 3. Plots of the experimental curve $f(V) = \ln(I/A^*ST^2)$ and the corrected curve with $R_s = 50\ \Omega$.

Pd/GaN contacts. It can be clearly seen from this figure that Pd/GaN SD has good rectifying properties at different temperatures and they are manifestly temperature-dependent. Clearly, by increasing the temperature, an increase of the current is observed as predicted by the thermionic emission model. Similar results were obtained for the other M/n-GaN SD, using either Pt or Ni as metal Schottky contacts. The forward I–V characteristics for all contacts studied were modeled using the following equations, which are consistent with thermionic emission theory.

$$I = A^*ST^2 \exp\left(-\frac{\Phi_{0Bn}}{k_BT}\right)\left[\exp\left(\frac{q(V - R_sI)}{nk_BT}\right) - 1\right] \quad (1a)$$

with

$$I_s = A^*ST^2 \exp\left(-\frac{\Phi_{0Bn}}{k_BT}\right), \quad (1b)$$

where I_s is the saturation current, Φ_{0Bn} the apparent barrier height at zero bias, A^* the modified Richardson constant, which is equal to 26.9 A cm^{-2} K^{-2} for M/n-type GaN Schottky contacts [20][1], S the area of the diode, T the temperature of the M/Sc junction, k_B the Boltzmann constant, n the ideality factor of the diode, R_s the series resistance and V is the forward applied bias. For each temperature, the experimental I–V data is used to extract the series resistance and the fundamental Schottky parameters (apparent barrier height and ideality factor). The series resistance R_s was determined using the Werner method [21]. Under forward bias, for $V - R_sI \gg (nk_BT/q)$, equations (1*a*) and (1*b*) yield the following function $f(V)$.

$$f(V) = Ln\left(\frac{I}{A^*ST^2}\right) = \frac{q}{k_BT}\frac{(V - R_sI)}{n} - \frac{\Phi_{0Bn}}{k_BT}. \quad (2)$$

The determined series resistance is introduced in equation (2) and then by plotting $f(V)$ as function of $V - R_sI$, the ideality factor n and Φ_{0Bn} at each temperature are extracted from the slope and the y-axis intercept, respectively. To illustrate that, an example of $f(V)$ versus $V - R_sI$ at 300 K for Pd/n-GaN SD is plotted in figure 3. The SBH can be also determined from reverse C–V characteristics; under reverse bias V_r, The zero barrier height Φ_{0Bn} is an apparent SBH which differs from the zero-field barrier Φ_{FBn} determined under flat band condition by C–V measurements. The C–V characteristic was also used

[1] Theoretical value of the effective Richardson constant $A^* = 4\pi m^* q k_B/h^3$ for the GaN sample used in this work is calculated to be 26.9 A cm^{-2} K^{-2} using the effective mass for electron $m^* = 0.22m_0$ (see for example [18] and [19]).

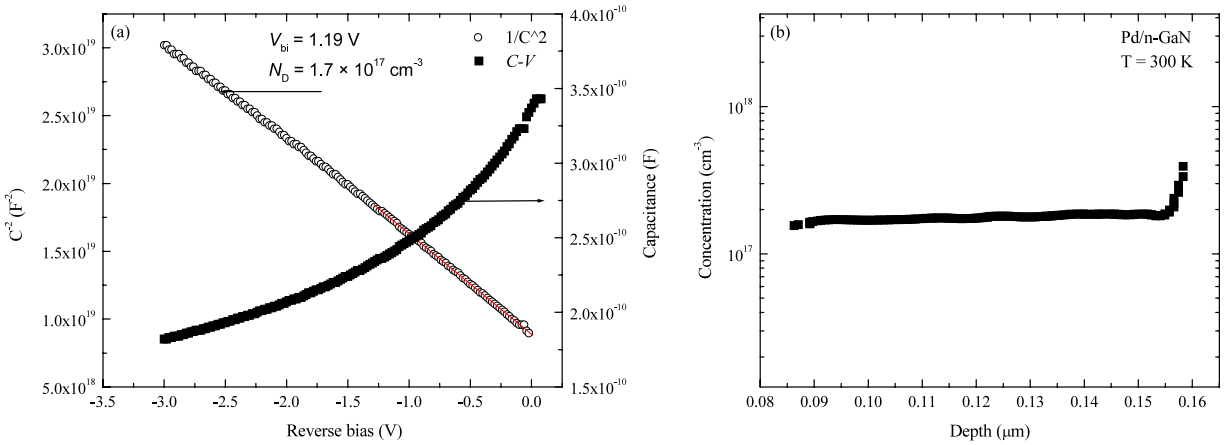

Figure 4. (a) C–V and $1/C^2$–V characteristics of Pd/n-GaN SD measured at 1 MHz. (b) Depth profile of electron concentration in Pd/n-GaN SD.

to determine the depth profile of the free carrier concentration. The measured capacitance is connected to the reverse applied voltage V_r [22] according to equation (3).

$$C_{mes} = \sqrt{\frac{S^2 \varepsilon_0 \varepsilon_{sc} q N_D}{(V_{bi} - V_r)}}, \tag{3}$$

where S, q and ε_0 have their usual definitions, N_D is the donor doping concentration, ε_{sc} the dielectric constant of GaN, which is equal to 9.5 [18], V_r the applied reverse bias and V_{bi} is the zero-bias built-in potential, which can therefore be determined from the flat band voltage V_{FB} for which $1/C^2 = 0$ holds. The reverse bias capacitance–voltage and $C^{-2} - V$ characteristics at 1 MHz and at 300 K plotted in figure 4(a) show an example of the result obtained for Pd/n-GaN SD. Under the applied reverse bias, the Pd electrode (Schottky contact) was negatively biased with respect to the electrode of the ohmic contact. The SBH deduced from CV measurements gives the zero-field barrier which corresponds to the flat band conditions Φ_{FBn}:

$$\Phi_{FBn} = \Phi_{BC-V} = q V_{bi} + k_B T \ln\left(\frac{N_C}{N_D}\right). \tag{4}$$

Here N_C is the effective density of states in the conduction band and N_D is the donor doping concentration, which is determined from the slope of $1/C^2$ plot according to equation (3). The slope in figure 4(a) was extracted to be -7.4×10^{18} F^{-2} V^{-1}. This corresponds to a uniform donor impurity concentration in the GaN film of 2×10^{17} cm^{-3}. The intercept at the voltage axis was determined to be 1.2 V. This corresponds to an SBH at flat band condition of 1.26 eV. The RT donor carrier concentration as function of junction depth is given in figure 4(b). It is clear from this figure that the doping concentration is uniform over a large depletion width. The SBH values determined from C–V measurement are always higher than those derived from I–V measurements. This point will be discussed later.

3.2. Interface states density

The existence of an interfacial layer between metal and Sc, (native oxide, metallization-induced modification/defects, residual structural defects in the Sc, etc) transform the metal-Sc structure onto metal-interfacial layer-Sc (MIS) diode. With such an interfacial layer, electronic surface states are created at the interface between the interfacial layer and the surface of the Sc. In this case the ideality factor and the SBH will consequently deviate from those expected for an ideal SD. Discussions related to the presence of the thin interfacial layer film [23, 24], usually starting with the assumption that the interfacial layer is sufficiently thick, and interface states, which depend only on the semiconductor, are in equilibrium with the Sc. For a thick enough interfacial layer separating the metal from the semiconductor, the transmission probability between the metal and the interface states that are located at the Sc-interfacial layer interface is very small. The bias dependence of the SBH is described in terms of the dependence of the ideality factor n on the applied bias due to surface states, and the barrier height shift with forward bias V, is given by equation (5) [23, 25]

$$\Phi_e(V) - \Phi_{0Bn} = q\left(1 - \frac{1}{n(V)}\right)(V - R_s I). \tag{5}$$

The ideality factor as introduced in equation (1) can be directly determined for each measuring temperature at any given forward bias from the slope of the semi-logarithmic I–V characteristics: $n(V) = \frac{q}{k_B T}\frac{dV}{d(\ln I)}$. Figure 5 shows an example of the forward bias-dependent ideality factor $n(V)$ at various temperatures taken from the experimental temperature-dependent $\ln(I)$–V characteristics of Pd/n-GaN SD given in figure 2. Figure 5 clearly shows that the ideality factor is a slowing varying function of the forward bias in the region where the effect of the series resistance ($R_s I$) is small (e.g. linear region of $\ln(I)$–V), followed by a large varying function of the forward bias where the effect of the series resistance dominates the $\ln(I)$–V characteristics. The latter effect gives rise to the curvature at higher current in the semi-log I–V plot. However the semi-log I–V plot has been divided into three different parts: the low forward bias region where the recombination current can dominate the current flow, the linear region where the thermionic emission assumption can

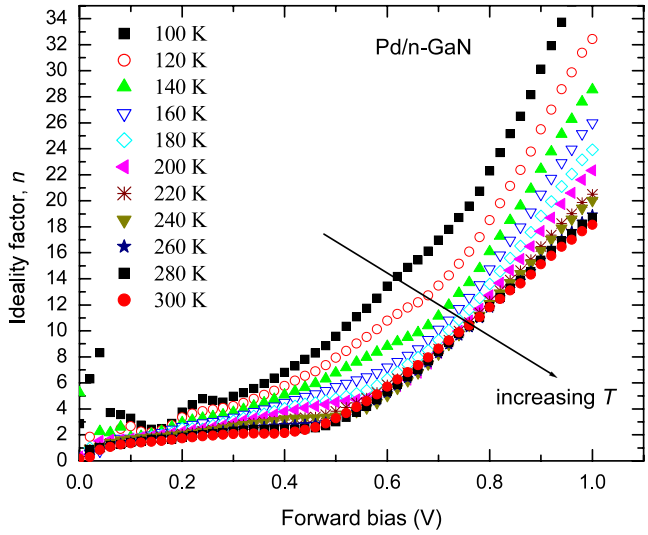

Figure 5. Plots of the forward bias-dependent ideality factor $n(V, T)$ for Pd/n-GaN SD at various temperatures.

be still valid and the upper current range where the series resistance effect dominates. Our data clearly indicate that the diode has ideality factor values larger than unity in the linear region. The bias dependence of the ideality factor, which is determined from the slope of the linear region of the semi-log I–V plot, is less pronounced as compared to that obtained from the upper region, at which the high bias voltage may remarkably modify the actual rectifying junction like behavior and lead to a very larger value of ideality factor without any physical meaning. An ideality factor larger than unity in the linear region of the semi-log I–V plot is generally attributed to specific interface structure states [23–26]. Moreover, when considering the temperature dependence of ideality factor at a given voltage, our data clearly indicate that the ideality factor increases with decreasing temperature. Similar results are obtained for Ni/n-GaN and Pt/n-GaN SDs: the ideality factor increases with increasing forward bias and decreases with increasing temperature.

The ideality factor, which is bias and temperature dependent, is related to the interfacial layer thickness and interface states density by the relation [26].

$$n(V, T) = 1 + \frac{\delta}{\varepsilon_0 \varepsilon_i}\left[\frac{\varepsilon_0 \varepsilon_{sc}}{w_{0D}} + q^2 N_{ss}(V, T)\right], \qquad (6)$$

where w_{0D} is the width of the depletion layer at zero voltage, N_{ss} the density of interface states, ε_0 the permittivity in vacuum, ε_i and ε_{sc} are the dielectric constants of the interfacial layer of thickness δ and the semiconductor, respectively. For an n-type semiconductor, the energy of interface states E_{ss} with respect to the minimum of conduction band E_C at the surface of the Sc is determined by using equation (7).

$$E_C - E_{ss} = (\Phi_e - qV). \qquad (7)$$

By using equations (5) and (6) together with equation (7) the interface states density N_{ss}, its distribution in the band gap at given temperature (spectral density $N_{ss}(E)$), and its variation as function of temperature at a given bias are determined. The depletion layer width w_{0D} at zero bias was found to be 0.1 μm (see figure 4(b)) and is temperature independent. The thickness of the interfacial layer was taken to be ∼2 nm. The interface states density is extracted by using the ideality factor values, as determined from the linear region of forward $\ln(I)$ versus $(V - R_s I)$ characteristics where the forward applied voltage $V \gg 3k_B T/q$. A typical result of $N_{ss}(E)$ at RT is shown in figure 6(a). As can be seen from figure 6(a), the N_{ss} value at RT for Pd/n-GaN SD decreases with increasing $E_C - E_{ss}$ value. It varies from 3×10^{13}(eV^{-1} cm^{-2}) at $E_C - 0.5$ eV to 3×10^{12} (eV^{-1} cm^{-2}) at $E_C - 0.63$ eV. The non-uniform distribution of $N_{ss}(E)$ is supposed to be due to the presence of discrete deep levels which are associated to the residual defects in the as grown GaN films. These defects are usually believed to be positioned away from the M/Sc interface. In such case, the interfacial layer separating the metal from the defects is the Sc itself. Moreover, the density of deep levels associated to native defects is supposed to peak at the energetic positions of the defect with respect to the band edge of the GaN film (i.e. defect concentration varies with energy and it is maximum at the energy position of the defects). This in turn indicates that the non-uniform distribution of the density of deep defects introduces a non-uniform lateral distribution of gap states at the metal/GaN interface. Accordingly, the density of surface states associated to defects will peak at the energy positions of these defects. DLTS measurements confirmed the presence of two major native defects D1 and D2 in the as grown GaN, as shown in figure 6(b) [27]. From comparison with the literature, it appears that the defect D2 under typical DLTS recording conditions (emission rate 200–220 s^{-1}) is the same as E_2 observed by Götz *et al* in n-GaN grown MOCVD epitaxy [28], as well as $E2$ located at 0.58 eV below E_C and EO5 located at 0.61 eV below E_C observed by Hacke *et al* and Goodman *et al* in vapor-phase epitaxially (VPE) grown GaN, respectively [29]. This defect was observed at $E_C - 0.61$ eV below the conduction band and may correspond to a nitrogen-related energy level [29]. From the peak temperatures of D1, it seems that defect D1 is presumably the same as defect $E3$ detected in as grown hydride vapor-phase epitaxially grown material [29] and ER4 observed after particle irradiation [30]. The energy level of ER4 was observed at $E_C - 0.78$ eV below the conduction band and the nature of the defect is as yet unresolved. Furthermore, figure 6(c) shows the temperature dependence of N_{ss} for Pd/n-GaN SDs at fixed forward bias, which corresponds to an energy of interface states of 0.57 eV with respect to the bottom of the conduction band, E_C. The variation of N_{ss} with energy up to 0.57 eV below the conduction band is observed to be weakly temperature-dependent. Such a small variation of the surface states density N_{ss} with temperature will induce a slight shift to higher values as the temperature decreases. A similar observation has been made elsewhere for other M/Sc contacts [31, 32]. Variation of the Schottky barrier height as a function of metal work function is also used to determine the surface states density. The Schottky contacts to n-GaN for a variety of elemental metals have been studied extensively [18, 33–35]. The reported Schottky barrier height

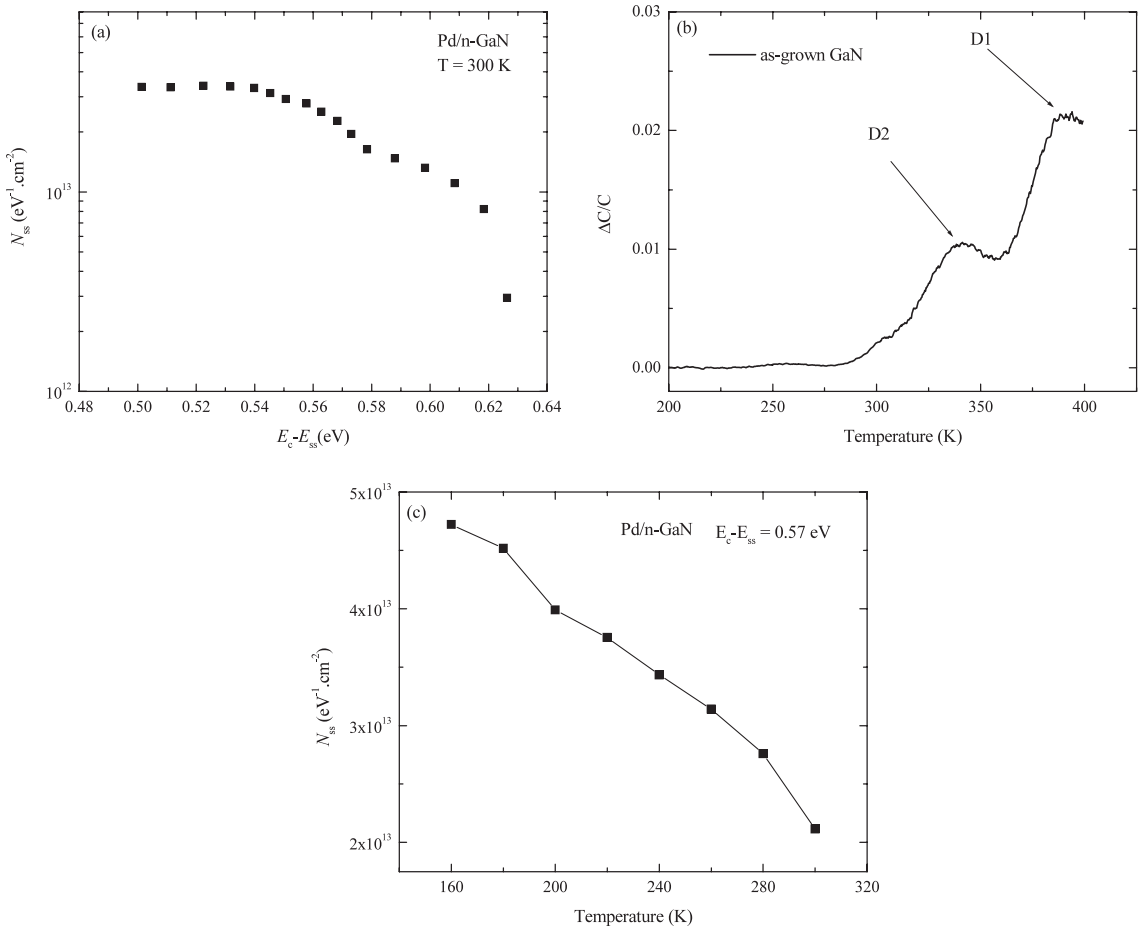

Figure 6. Surface states energy distribution $N_{ss}(E)$ at the Pd/n-GaN interface (a). (b) and (c) are the variation of the surface states density as a function of temperature and the DLTS spectrum of SBD on n-GaN, respectively.

increases monotonically but with a considerable amount of scatter in the experimental data for a given metal. However, it scales proportionally with metal work function, although the coefficient of proportionality deviates from unity as predicted by the Schottky–Mott Model. One of the important issues in investigating the dependence of the SBH of M/n-GaN on Φ_M is to determine the interface behavior parameter ($\gamma = \frac{\partial \Phi_{0Bn}}{\partial \Phi_M}$) and determine whether the Fermi level is pinned with respect to one of the band edges. It is argued that, due to the substantial ionic component of the bonds in III–V nitrides, the Fermi level at the nitride surface and at the metal–nitride interface should be unpinned [36, 37]. Because of the presence of an interfacial thin layer, which separates the Sc and the metal, the net charge of the gap states together with its image charge on the surface of the metal will form a dipole layer. This dipole layer will alter the energy barrier and therefore the Φ_{0Bn} depending on the surface states density and on the metal work function according to equation (8).

$$\Phi_{0Bn} = \gamma(\Phi_M - \chi_S) + (1-\gamma)(E_g - \Phi_0) = \gamma(\Phi_M - \chi_S) + \beta \quad (8)$$

where Φ_0 is the charge neutrality level (CNL) position with respect to the valence band maximum and γ and β are two structural constants; γ is given by:

$$\gamma = \frac{\varepsilon_i}{\varepsilon_i + q^2 N_{ss}\delta}, \quad (9)$$

where ε_i and δ have been defined before as the permittivity and the thickness of interfacial layer, respectively. Two sets of results will be presented here. The first one is focused on the determination of N_{ss} from the dependence of SBH on metal work function. The second one is to compare the above determined N_{ss} to that determined from the experimental data of the forward bias I–V characteristics. Figure 7 shows $\ln(I/A^*ST^2)$ versus $V - R_s I$ plot at RT for the three different SDs corresponding to three different metal work functions Φ_M, (Pd, Ni, Pt). As can be clearly seen from this figure, the y-axis intercept ($V = 0$) changes with Φ_M, while the slope of the three I–V curves does not change with Φ_M. This result shows that the SBH increases with increasing Φ_M. In fact the SBH depends on the work function as expected but does not scale as predicted by the Schottky–Mott Model with a unity coefficient of proportionality. The variation of the SBH on n-GaN as function of Φ_M is plotted in figure 8. Literature values of SBH as a function of Φ_M for metal contacts on GaN including Ti, Cr, Ag, Au, and Pt [9, 15, 38–42] are also reported in this figure. The BH of Pt/n-GaN SD, obtained in

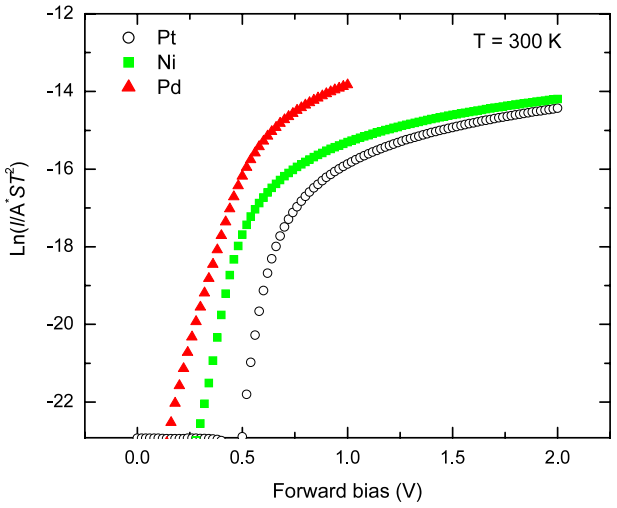

Figure 7. Room temperature plot of $\ln(I/A^*ST^2)$ versus $V - R_sI$ for Pd, Ni and Pt Schottky contacts on n-GaN.

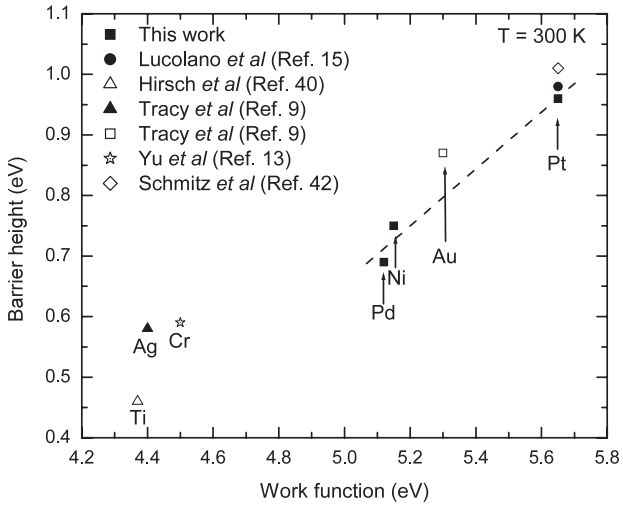

Figure 8. Variation of the zero-bias SBH as a function of metal work function. Data from this work (full square). Literature values of SBHs as a function of Φ_M for contacts on n-GaN with Ti (open triangle) (see [39]), Pt (full circle and open rhombus) (see [15, 41]), Au (open square) (see [9]), Cr (open star) (see [13]), Ag (full triangle) (see [9]).

this work, is comparable to BH values reported by Iucolano *et al* and Schmitz *et al* [15, 41]. Moreover, the SBH is found to have a dependence on the metal work function and, indeed, a roughly linear relationship between Φ_{0Bn} and Φ_M is observed. Although a monotonic increase in SBH is observed as Φ_M is increased, there is a contribution from the defects states and/or MIGS. A slope of ∼0.47 is deduced from the straight line fitted to the experimental values, which agrees with that reported by Tracy *et al* [9]. This interface parameter is used to calculate the interface states density, while the extrapolated value through the SBH axis is used to determine the charge neutrality energy level at surface, Φ_0 above the valence band. An average density of surface states $N_{ss} \approx 3.3 \times 10^{13}$ eV^{-1} cm^{-2} at $T = 300$ K is deduced from the gap states parameter, $\gamma \sim 0.47$ (see equations (8) and (9)), by taking the total per-area charge of the gap states to be positioned at distance, $\delta \approx 2$ nm, away from the interface, and by considering that the dielectric constant of the interface region is $\varepsilon_i/\varepsilon_0 \approx 9.6$. This value is comparable to the energy-averaged value of $N_{ss}(E)$ measured (over the range of 0.5–0.6 eV below E_C) from the bias dependence of ideality factor, as determined from the experimental data of the forward bias I–V characteristics at $T = 300$ K. This result suggests that the surface gap states at the M/Sc interface are a property of only the semiconductor, and not the metal. Using Schottky capacitance spectroscopy, a similar result of interface state density was obtained by Iucolano *et al* [42], who also observed that N_{ss} at the Ni/n-GaN interface increases upon thermal annealing. However, the preliminary result reported in the present work supports the tentative proposition that the interface gap states are associated to the native defects in the as grown GaN film and the sources of gap states are defect related states. The contribution of MIGS to the surface states density cannot be ruled out. It should be also noted that the CNL position, Φ_0 as determined from this research work, is about 0.45 eV below the conduction band.

According to Schottky–Mott theory, the SBH between a metal with work function Φ_m and a Sc with an electron affinity of χ_{sc} should be

$$\Phi_{0Bn} = \Phi_M - \chi_{sc}. \tag{10}$$

By substituting the value of the electron affinity of GaN (4.1 eV) and Φ_m for Pd, Ni and Pt in equation (10), the interface dipole contribution can be estimated by taking the difference between the calculated Schottky–Mott barrier height and the experimentally measured SBH. As a result, an interface dipole contribution of 0.33, 0.29 and 0.56 eV is determined for Pd, Ni and Pt/n-GaN SDs, respectively. The values of interface dipole contribution are in good agreement with those previously published for Pt/GaN (0.55 eV) and Ni/GaN (0.25 eV) (see [9]). The difference in the interface dipole contribution for the different metals deposited on identically prepared GaN surface could be attributed to the contribution from MIGS due to the low screening in GaN [43].

3.3. Barrier inhomogeneities

The experimental values of n and SBH, as well as their irrespective temperature dependence, reflects the departure from ideality; namely the larger the ideality factor n, the larger deviation from the ideal behavior of the SD. In general, the temperature dependence of the I–V characteristics allows us to determine the conduction process as well as the nature of barrier formation at the M/n-GaN interface [44, 45]. The temperature dependence of the ideality factor and the SBH determined from I–V–T curves for both Pd/n-GaN and Pt/n-GaN are shown in figures 9(a) and (b). Above 180 K, the variations of the SBH and the ideality factor with temperature are limited. Below 180 K, a respective increase and decrease of the ideality factor and the barrier height is observed with decreasing temperature. Similar trends have already been reported for contacts on other semiconductors. The decrease in the SBH and the increase in ideality with a

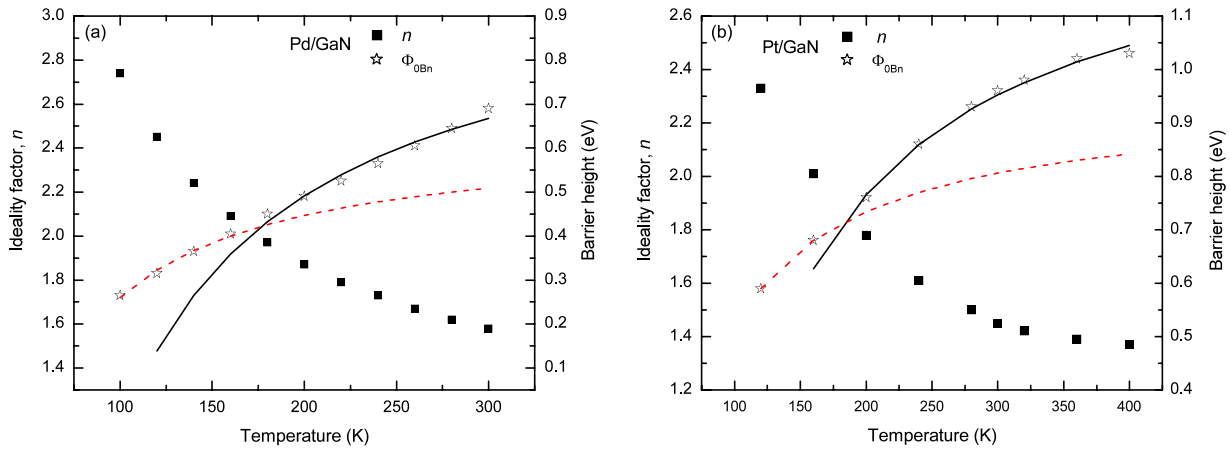

Figure 9. Zero-bias SBH and ideality factor as a function of temperature for Pd/n-GaN (a) and Pt/n-GaN (b). Broken and solid lines without symbols are for the calculated SBHs using equation (11) for two Gaussian distributions of BHs in the temperature ranges (80–160 K: distributions (2)) and (160–400 K: distribution 1), respectively.

decrease in temperature can be explained by assuming lateral inhomogeneities of SBH at the interface [46, 47], with a Gaussian spatial distribution of SBHs around zero-bias of mean value $\bar{\Phi}_{0Bn}$ and with a zero-bias standard deviation σ_{0s}. According to the Werner–Güttler model [46] and for thermodynamic equilibrium ($V = 0$), the barrier height of the spatial inhomogeneous Schottky contact will have a temperature dependence which can be described by the following equation [46]:

$$\Phi_{0Bn} = \bar{\Phi}_{0Bn} - \frac{\sigma_{0s}^2}{2k_BT}, \tag{11}$$

where Φ_{0Bn} is the apparent SBH measured experimentally at 0 V. It is worth noting that the SBH value derived from I–V measurements is smaller than the SBH value extracted from C–V measurement. This is due to the different nature of the I–V and C–V measurement techniques. The capacitance C is insensitive to potential fluctuations on a length scale of less than the space charge region and the C–V method averages over the whole Schottky area and results in a homogeneous SBH [47]. The DC current I across the interface depends exponentially on barrier height and thus sensitively on the detailed distribution of surface states density at the interface. According to equation (11), the plot of Φ_{0Bn} versus $1/2k_BT$ should be a straight line with the intercept at the ordinate determining the zero-bias mean value of SBH, $\bar{\Phi}_{0Bn}$, and the slope giving the zero-bias standard deviation, σ_{0s}. For both Pd/n-GaN and Pt/n-GaN SDs, the experimental Φ_{0Bn} versus $1/2k_BT$ plots (see figure 10) can be described by two straight lines, instead of a single straight line, with a transition occurring at 160 K. The above observation may indicate the presence of two Gaussian distributions of SBHs over the Schottky contact area. For a Pd/n-GaN SD (figure 10(a)), the intercepts and slopes of these straight lines give the two sets of values, $\bar{\Phi}_{0Bn}$ and σ_{0s} as 1.02 and 0.14 eV in the temperature range of 160–300 K (distribution 1), and 0.63 and 0.077 eV in the temperature range of 100–160 K (distribution 2). On the other hand, for the Pt/GaN SD (figure 10(b)), the values of $\bar{\Phi}_{0Bn}$ and σ_{0s} were determined as 1.32 and 0.14 eV in the temperature range of 160–400 K (distribution 1), and as 0.96 and 0.086 eV in the temperature range of 120–160 K (distribution 2). The existence of a double Gaussian on M/Sc Schottky diodes was already experimentally proven by I–V – T measurements and BEEM [48, 49]. For a comparison purpose, calculated SBHs, for Pd/GaN and Pt/GaN SDs (using equation (11) for two Gaussian distributions of BHs with the experimentally obtained values of $\bar{\Phi}_{0Bn}$ and σ_{0s}) are also shown in figure 9. It is evident from figure 9 that the temperature dependence of the experimental values of SBH of Pd/GaN and Pt/GaN can be described by two Gaussian distributions in the temperature range 80–400 K. Moreover, the large values of the standard deviation are usually an indication of large degree of inhomogeneities at our M/GaN Schottky contacts. It is worth noting that the two standard deviation values obtained for Pd/n-GaN SD are similar to those obtained for Pt/n-GaN SD. Therefore, the above result again suggests that the origin of barrier inhomogeneity in M/GaN SD is a property of the Sc and does not depend on the deposited metal. Other possible origin of the deviation from linearity at low temperature, such as quantum tunneling including thermionic field emission (TFE) and edge effects due to device periphery cannot be ruled out. Because of the low TE current level in the wide band gap Sc (GaN) at low temperature, another current component than TE, such as TFE and carrier recombination, might dominate the carrier transport at low temperature. On the other hand, the edge effect, which is connected to the device periphery, becomes dominant at low temperature in comparison to the total diode current, i.e. the leakage current due to the edge effect can therefore contribute to the TE currents at low temperature.

The activation energy of $\ln(I_s/T^2)$ versus $1/k_BT$ allows the determination of the effective SBH according to equation (1*b*). From the experimental data reported in figure 2, the value of the saturation current I_s is determined at each temperature and conventional Richardson plots, $\ln(I_s/T^2)$ versus $1/k_BT$ (indicated by solid squares) for Pd/n-GaN and for Pt/n-GaN SDs, are reported in figures 11(a) and (b), respectively. An experimental $\ln(I_s/T^2)$ versus $1/k_BT$ plot

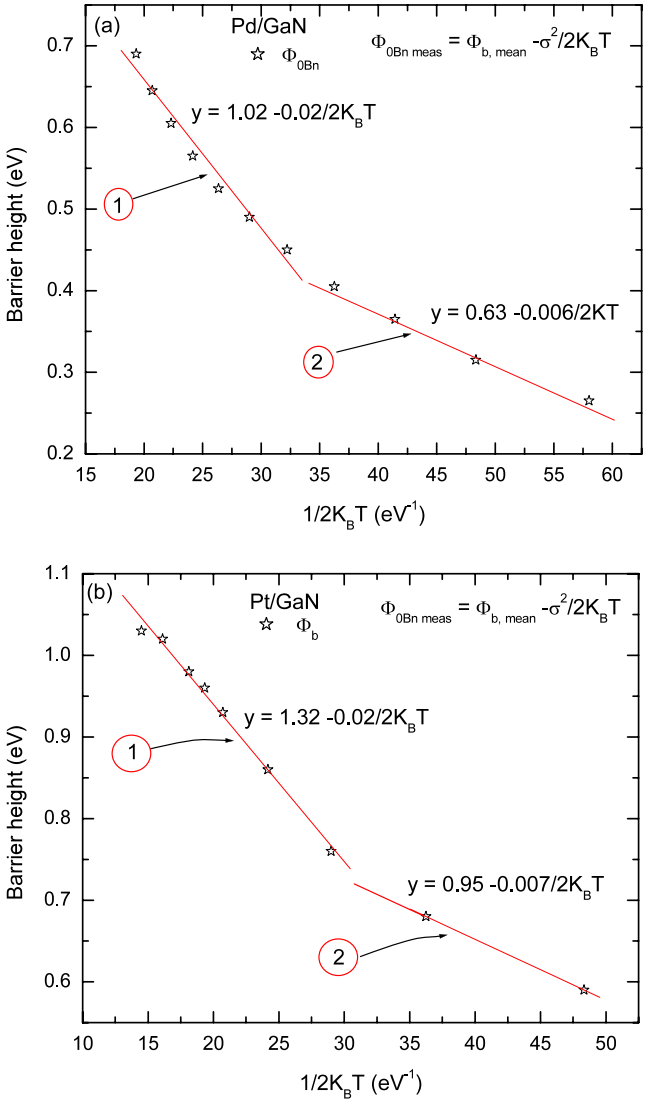

Figure 10. Experimental zero-bias SBHs versus $1/2k_BT$ curves of Pd/n-GaN (a) and Pt/n-GaN (b) Schottky diodes according to the Gaussian distributions of SBHs. The experimental data is described by two straight lines with a transition at 160 K.

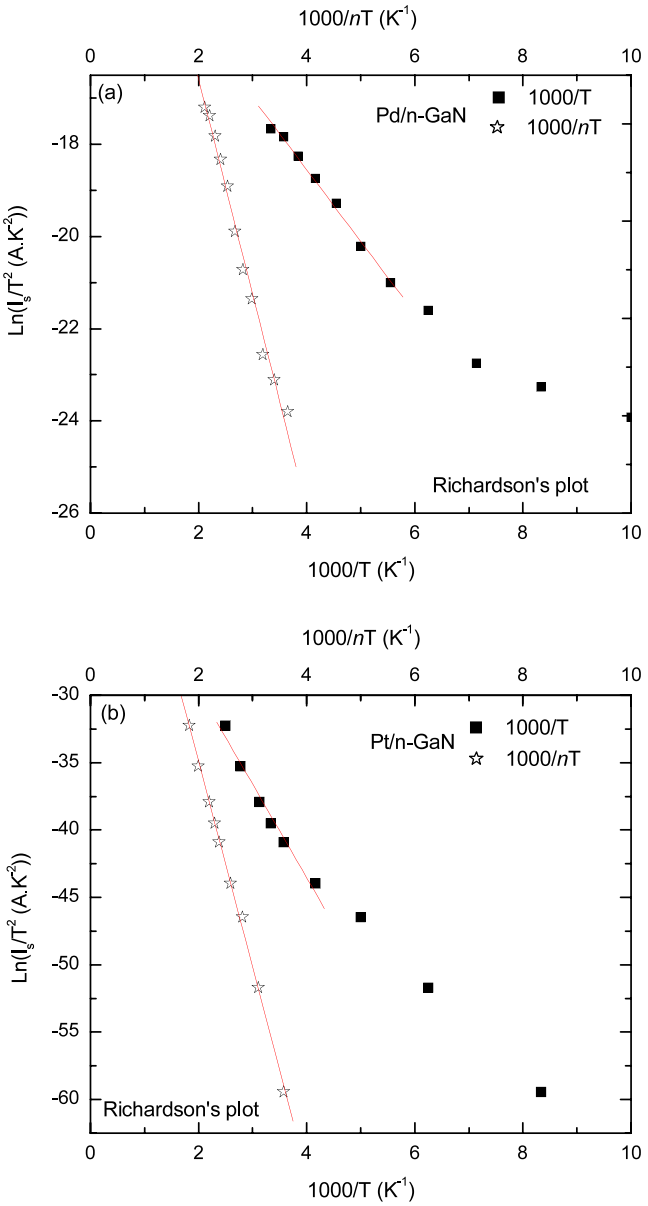

Figure 11. Richardson plot, $\ln(I_s/T^2)$ versus $1000/T$ and modified Richardson plot $\ln(I_s/T^2)$ versus $1000/nT$ for Pd/n-GaN (a) and Pt/n-GaN (b) Schottky diodes.

should give a straight line with a slope given by an SBH at 0 K, $\Phi_{0Bn}(T = 0)$ and an intercept at the ordinate given by an experimental Richardson's constant, A^*. When trying to fit the experimental data, a distortion of the curve is clearly visible at low temperatures for both Schottky devices. From this fit, SBHs $\Phi_{0Bn}(T = 0)$ of 0.13 eV and 0.6 eV and Richardson's constants values of $A^* = 1.3 \times 10^{-3}$ A cm^{-2} K^{-2} and 4.1×10^{-5} A cm^{-2} K^{-2} were extracted for Pd/n-GaN and Pt/n-GaN, respectively.

The significant deviation from linearity of the experimental $\ln(I_s/T^2)$ versus $1/k_BT$ curve is caused by the temperature dependence of the SBH and ideality factor. As explained above, the non-ideality for both Schottky devices can be due to another transport mechanism in addition to the TE at low temperature and/or to the so-called edge effect, which cause departure from thermionic emission behavior at low temperature. In order to take into account the experimentally observed temperature-dependent ideality factor, a modified Richardson's plot $\ln(I_s/T^2)$ versus $1/nk_BT$ is also reported in figures 11(a) and (b) for both SDs. The linear behavior of $\ln(I_s/T^2)$ versus $1/nk_BT$ displayed in figure 11 gives a better fit to the experimental data over the whole temperature range, giving SBHs $\Phi_{0Bn}(T = 0)$ of 0.41 eV and 1.3 eV and Richardson's constants of $A^* = 0.2$ A cm^{-2} K^{-2} and 3.4 A cm^{-2} K^{-2} for Pd/n-GaN and Pt/n-GaN SDs, respectively. The latter values of Richardson's constant are still lower than the theoretical values [20] (see footnote 1). The large difference in the Richardson's constant value as determined for Pd/n-GaN and Pt/GaN SDs can be ascribed to the nature of the metal or to the different metal deposition technique used to fabricate the Pd/n-GaN (thermal evaporation) and Pt/n-GaN (e-beam deposition) SDs. The latter result has to be further investigated. However, it

is to be noted that some authors have reported results that indicate that the Richardson constant could also depend on the metal [50].

The SBH inhomogeneities may occur as a result of the poor interface quality, which, in turn, depends on several factors such as the surface and bulk defects density distribution, the inhomogeneities in the interfacial thin layer stoichiometry, compositional changes at the near surface region, non-uniformity of the interfacial charges distribution, and interfacial layer thickness, etc. In such cases, the current flowing across the metal/GaN interface may strongly be influenced by the presence of the SBH inhomogeneities. From the present study, it can be argued that the laterally inhomogeneous SBH can be related to the non-uniform distribution of interface states density, which occurs as a result of the presence of native defects at and below the surface of GaN. Within this 'non-uniform distribution of $N_{ss}(E)$' model, the existence of two Gaussian distributions can be explained by the peak positions of $N_{ss}(E)$ at two discrete energy levels associated with the two defects D1 and D2.

As reported earlier, a dependence of both SBH and n on the temperature is commonly observed in real metal/Sc Schottky contacts and attributed to the non-homogeneous Schottky contacts. In fact the laterally homogeneous SBH of M/n-GaN Schottky contacts is expected to be obtained by extrapolation of the experimental $\Phi_{0Bn}(n)$ plots to $n = 1$ [51–53]. It should be noted that because of the double Gaussian distributions of the BHs at M/GaN SD, two sets of homogeneous SBH values, were obtained by extrapolation of the experimental $\Phi_{0Bn}(n)$ plots to $n = 1$ (not shown here). For Pd/n-GaN SD, values of 0.65 eV and 1.02 eV were obtained in the temperature range 80–160 K (distribution 2) and 160–300 K (distribution 1), respectively, while values of 0.99 eV and 1.27 eV were obtained for Pt/n-GaN in the temperature range 120–160 K (distribution 2) and 160–300 K (distribution 1), respectively.

If the non-uniform distribution of interface states density is considered as being the origin of the inhomogeneities of SBH, then the measured SBH must be more or less equal (by considering the image force lowering correction) to the homogeneous SBH barrier, provided the interface states density is very low. This must be verified by plotting the measured SBH as a function of the corresponding extracted interface states at different temperature. Figure 12(a) displays such a variation for Pd/n-GaN Schottky contacts. A dependence of SBH on the interface states density is clearly observed. However, this variation is correlated, in that the apparent barrier height becomes lower with increasing interface states density. In particular, an almost linear correlation between SBH and interface states density is obtained; the SBH increases linearly with decreasing interface states density with the intercept at the ordinate axis determining the image force controlled zero-bias homogeneous SBH. From the linear extrapolation of SBH versus N_{ss} plots to $N_{ss} \sim 0$, a SBH of 0.93 eV is obtained for Pd/n-GaN Schottky contacts. The extrapolated value of SBH is in reasonable agreement with the homogeneous SBH values obtained in the temperature range 160–300 K from the plots of Φ_{0Bn}

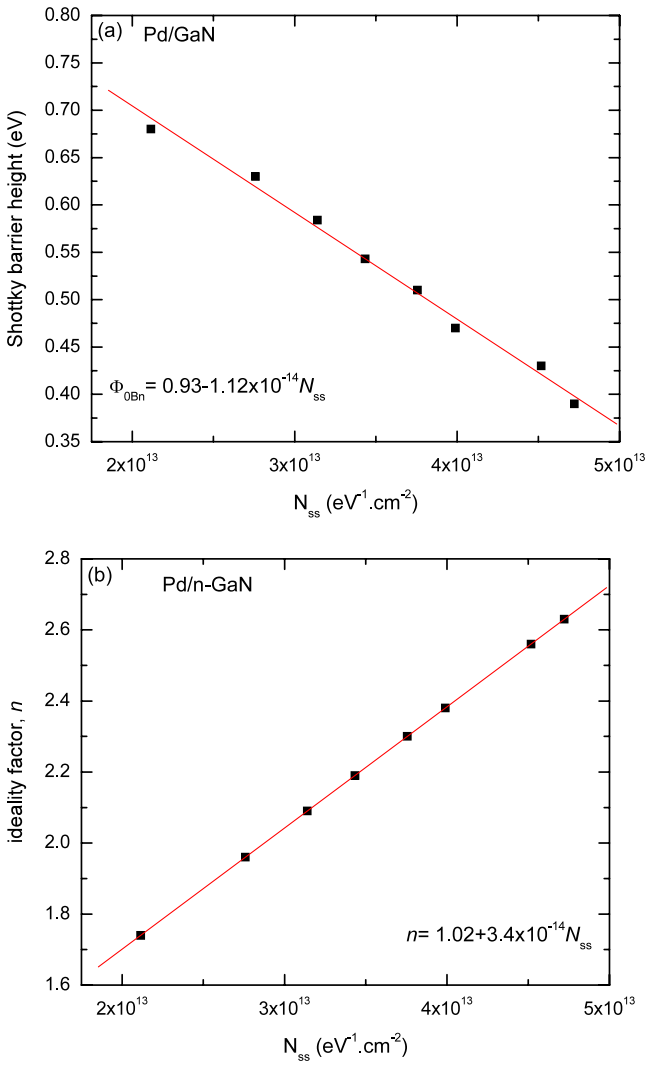

Figure 12. Zero-bias SBHs (a) and ideality factor (b) as a function of surface states density for Pd/GaN SD. A linear correlation can be seen between Schottky parameters (SBH and ideality factor) and surface states density.

versus n and Φ_{0Bn} versus $1/2k_BT$. The slight difference of 0.09 eV between the values of BHs of the homogeneous mean value (1.02 eV) and that (0.93 eV), extrapolated at $N_{ss} \sim 0$, from the $\Phi_{0Bn}(N_{ss})$ plot can be explained by the effect of image force lowering. In fact the linear extrapolation of the experimentally measured BH Φ_{0Bn} versus N_{ss} curves gives the image force-lowered barrier height of the laterally homogeneous contacts[2]. Similarly, the extrapolation of the linear fits of ideality factor, n versus N_{ss} (see figure 12(b)) to $N_{ss} \sim 0$, gives an ideality factor of 1.02, which corresponds to the image force controlled ideality factor (n_{if}) at homogeneous Schottky contacts. Interestingly, the rate at which Φ_{0Bn}

[2] The barrier height $\bar{\Phi}_{0Bn}$ of laterally homogeneous Pd/n-GaN SD is determined to be $\bar{\Phi}_{0Bn} = \Phi_{0Bn}(N_{ss} \to 0) + \Delta\Phi_{if}(0\ V) \sim 1$ eV. The zero-bias image force-lowered barrier height given by $\Delta\Phi_{if}(0\ V) = \sqrt{\frac{qE_m}{4\pi\varepsilon_0\varepsilon_{sc}}} = [\frac{q^3 N_D V_{bi}}{8\pi^2(\varepsilon_0\varepsilon_{sc})^3}]^{\frac{1}{4}}$ is calculated to be 0.07 eV for a doping concentration of $N_D = 2 \times 10^{17}$ cm^{-3} and a diffusion potential of $V_{bi} = 1.2$ V as determined in our Pd/n-GaN SDs (see [22], p. 251 and [23], p. 360).

and n vary with N_{ss} is approximately the same. These findings confirm the earlier prediction that the lateral barrier inhomogeneities at the M/GaN interface are connected to the non-uniformity distribution of $N_{ss}(E)$ at the M/GaN, which is attributed to the native defects at and close to the metal–GaN interface.

Thus, on the basis of the results presented above, deep levels associated with native defects D1 and D2 could be considered as the origin of the lateral inhomogeneity of the Schottky barrier height through the non-uniform energy distribution of interface trap states at the metal/GaN interface.

4. Conclusion

The Schottky barrier height and ideality factor of various metal/GaN Schottky contacts using Pd, Ni and Pt as metals have been studied as a function of the forward bias and temperature, covering the temperature range 80–400 K, using current–voltage technique. The interface states density was extracted from both the forward bias dependence of the SBH and n for a given metal and from the SBH dependence of the metal work function at a given forward bias. A good correlation is found between the two ways of determining the interface states densities. Additionally, the zero-bias barrier heights and ideality factors of M/n-GaN are found to be strongly temperature-dependent with a decrease in the BH and an increase in the ideality factor with decreasing temperature. This temperature dependence of BH and ideality factor was satisfactorily explained by assuming the existence of double Gaussian distributions of the barrier height values in the temperature range 80–400 K, with the BH mean value of the second Gaussian being smaller than that of the dominant one. Furthermore, the laterally inhomogeneous contacts are found to be of the same kind, regardless the nature of the metal. Moreover a linear correlation between BH at zero bias and surface states density is observed. By using DLTS, it was found that two electrically active defects D1 and D2, with discrete energy levels, were introduced in the band gap of GaN. The present results lead to the conclusion that the origin of the lateral inhomogeneities of the Schottky barrier height is a property of only the GaN material and is associated to the non-uniform distribution of surface gap states at metal/GaN contacts, which could be attributed to the native defects D1 and D2 present in the as grown GaN film.

Acknowledgments

The author acknowledges the fruitful discussions of Dr A Mesli and Dr K Bouziane. The author would like also to thank B Al Hashmi for her contribution to this work and Dr A Sellai for making the I–V setup available for a portion of this work. This work is supported by Sultan Qaboos University under Contract No. IG/SCI/PHYS/08/02. A portion of this work was also done while the author was a visiting scientist at the Laboratory '*Centre de Recherche sur les Ions, les Matériaux et la Photonique* (CIMAP)' CNRS-ENSICAEN-CEA-UCBN, France.

References

[1] Morkoç H, Strite S, Gao G B, Lin M E, Sverdlov B and Burns M 1994 *J. Appl. Phys.* **76** 1363
[2] Jain S C, Willander M, Narayan J and Van Overstraeten R 2000 *J. Appl. Phys.* **87** 965
[3] Ambacher O 1998 *J. Phys. D: Appl. Phys.* **31** 2653
[4] Monemar B 1999 *J. Mater. Sci.: Mater. Electron.* **10** 227
[5] Spicer W E, Lindau I, Skeath P, Su C Y and Chye P 1980 *Phys. Rev. Lett.* **44** 420
[6] Cao R, Miyano K, Lindau I and Spicer W E 1989 *Thin Solid Films* **181** 43
[7] Tersoff J 1984 *Phys. Rev. Lett.* **52** 465
[8] Cowley A M and Sze S M 1965 *J. Appl. Phys.* **36** 3212
[9] Tracy K M, Hartlieb P J, Einfeldt S, Davis F R, Hurt E H and Nemanich R J 2003 *J. Appl. Phys.* **94** 3939 and references therein
[10] Lee M L, Sheu J K and Lin S W 2006 *Appl. Phys. Lett.* **88** 032103
[11] Wang L, Nathan M I, Lim T H, Khan M A and Chen Q 1996 *Appl. Phys. Lett.* **68** 1267
[12] Baranwal V, Kumar S, Pandey A C and Kanjilal D 2009 *J. Alloys Compounds* **480** 962
[13] Yu L S, Liu Q Z, Xing Q J, Qiao D J, Lau S S and Redwing J 1998 *J. Appl. Phys.* **84** 2099 and references therein
[14] Zhang H, Miller E J and Yu E T 2006 *J. Appl. Phys.* **99** 023703
[15] Iucolano F, Roccaforte F, Giannazzo F and Raineri V 2007 *Appl. Phys. Lett.* **90** 092119
[16] Iucolano F, Roccaforte F, Giannazzo F and Raineri V 2007 *J. Appl. Phys.* **102** 13701
[17] Wang L, Nathan M I, Lim T H, Khan M A and Chen Q 1996 *Appl. Phys. Lett.* **66** 1267
[18] Hacke P, Detchprohm T, Hiramatsu K and Sawaki N 1993 *Appl. Phys. Lett.* **63** 2676
[19] Ruvimov S, Liliental-Weber Z, Washburn J, Duxstad K J, Haller E E, Fan Z-F, Mohammed S N, Kim W, Botchkarev A E and Morkoç H 1996 *Appl. Phys. Lett.* **69** 1556
[20] Witowski A M, Pakuła K, Baranowski J M, Sadowski M L and Wyder P 1999 *Appl. Phys. Lett.* **75** 4154
[21] Werner J H 1988 *Appl. Phys.* A **47** 291
[22] Sze S M 1981 *Physics of Semiconductor Devices* 2nd edn (New York: Wiley)
[23] Rhoderick E H and Williams R H 1988 *Metal Semiconductor Contacts* (Oxford: Clarendon)
[24] Chattopadhyar P and Daw A N 1986 *Solid State Electron.* **29** 555
[25] Türüt A 1995 *Physics* B **205** 41
[26] Card H C and Rhoderick E H 1971 *J. Phys. D: Appl. Phys.* **4** 1589
[27] Mamor M, Matias V, Vantomme A, Colder A, Marie P and Ruterana P 2004 *Appl. Phys. Lett.* **85** 2244
[28] Götz W, Johnson N M, Amano H and Akasaki I 1994 *Appl. Phys. Lett.* **65** 463
[29] Goodman S A, Auret F D, Legodi M J, Beaumont B and Gibart P 2001 *Appl. Phys. Lett.* **78** 3815
Hacke P, Detchprohm T, Hiramatsu K, Sawaki N, Tadatomo K and Miyake K 1994 *J. Appl. Phys.* **76** 304
[30] Auret F D, Goodman S A, Koschnick F K, Spaeth J M, Beaumont B and Gibart P 1999 *Appl. Phys. Lett.* **74** 407
[31] Mamor M and Sellai A 2008 *J. Vac. Sci. Technol.* A **26** 705
[32] Sellai A, Mamor M and Al-Harthi S 2007 *Surf. Rev. Lett.* **14** 765
[33] Guo J D, Feng M S, Guo R J, Pan F M and Chang C Y 1995 *Appl. Phys. Lett.* **67** 2657
[34] Binari S C, Dietrich H B, Kelner G, Rowland L B, Doverspike K and Gaskill D K 1994 *Electron. Lett.* **30** 909
[35] Kribes Y, Harrison I, Tuck B, Cheng T S and Foxon C T 1997 *Semicond. Sci. Technol.* **12** 913

[36] Foresi J S and Moustakas T D 1993 *Appl. Phys. Lett.* **62** 2859
[37] Kurtin S, McGill T C and Mead C A 1969 *Phys. Rev. Lett.* **22** 1433
[38] Liu Q Z and Lau S S 1998 *Solid State Electron.* **42** 677
[39] Hirsch M T, Duxstad K J and Haller E E 1997 *Electron. Lett.* **33** 3108
[40] Kalinina E V, Kuznetsov N I, Dmitriev V A, Irvine K G and Carter C H 1995 *J. Electron. Mater.* **25** 831
[41] Schmitz A C, Ping A T, Khan M A, Chen Q, Yang J W and Adesida I 1996 *Semicond. Sci. Technol.* **11** 1464
[42] Iucolano F, Roccaforte F, Giannazzo F and Raineri V 2008 *J. Appl. Phys.* **104** 093706
[43] Picozzi S, Continenza A, Satta G, Massidda S and Freeman A J 2000 *Phys. Rev.* B **61** 16736
[44] Roccaforte F, La Via F, Raineri V, Pierobon R and Zanoni E 2003 *J. Appl. Phys.* **93** 9137
[45] Zhu S, Van Meirhaeghe R L, Detavernier C, Cardon F, Forment S, Ru G P, Qu X P and Li B Z 2000 *Solid-State Electron.* **44** 663
[46] Werner J H and Güttler H H 1991 *J. Appl. Phys.* **69** 1522
[47] Tung R T 1992 *Phys. Rev.* B **45** 13509
[48] Jiang Y L, Ru G P, Lu F, Qu X P, Li B Z and Yang S 2003 *J. Appl. Phys.* **93** 866
[49] Vanalme G M, Goubert L, Van Meirhaeghe R L, Cardon F and van Daele P 1999 *Semicond. Sci. Technol.* **14** 871
[50] Missous M and Rhoderick E H 1991 *J. Appl. Phys.* **69** 7142
[51] Akkiliç K, Türüt A, Çankaya G and Kiliçoğlu T 2003 *Solid State Commun.* **129** 551
[52] Schmitsdorf R F, Kampen T U and Mönch W 1995 *Surf. Sci.* **324** 249
[53] Mamor M, Sellai A, Bouziane K, Al Harthi S, Al Bousaidi M and Gard F S 2007 *J. Phys. D: Appl. Phys.* **40** 1351